Publishing Excellence Inspiring Progress
ARISTON PUBLICATIONS
MatSci Express
ISSN: 2997-8440 www.aristonpubs.com/matsci-express https://doi.org/10.69626/mse.2026.0033

RESEARCH ARTICLE

Effect of Tin Incorporation on Structural, Optical and Electrical Properties of Zinc Selenide Thin Films Prepared by Chemical Bath Deposition Method

T. A. H. Mir [1,*], A. U. Sonawane[2]

ABSTRACT: This study investigates the influence of tin (Sn) incorporation at varying concentrations (0%, 2%, 4%, and 6%) on the structural, optical, and electrical properties of zinc selenide (ZnSe) thin films synthesized via chemical bath deposition. Structural analysis reveals that increasing tin content leads to a significant narrowing of the dominant diffraction peak, indicating enhanced crystallinity and grain growth. Energy-dispersive X-ray spectroscopy (EDAX) confirms the presence of Sn, Zn, and Se, validating successful tin incorporation into the ZnSe lattice. Optical characterization demonstrates a systematic increase in absorbance with higher tin concentrations, accompanied by a reduction in the optical bandgap from 2.57 eV to 2.38 eV. Electrical measurements reveal a notable decrease in resistivity from 10^6 Ω.cm to 10^3 Ω.cm with increasing tin content, suggesting improved conductivity. These findings highlight the potential of tin-doped ZnSe thin films for optoelectronic applications, offering tunable optical and electrical properties through controlled tin incorporation.

Keywords: Chemical Bath Deposition, Tin Incorporation, Optical Analysis, Electrical Resistivity.

Received: 13 November 2025; Revised: 30 December 2025; Accepted: 17 January 2026; Published Online: 03 February 2026

1. INTRODUCTION

Zinc selenide (ZnSe) is a versatile semiconductor material with significant potential for applications in optoelectronics, including heterojunction solar cells, light-emitting diodes (LEDs) [1], photodiodes [2, 3], anti-reflective coatings [4], and dielectric mirrors [5]. The performance of these devices is heavily influenced by the optical and electrical properties of the thin films, which can be tailored through the incorporation of foreign atoms. Doping with elements having fewer or extra valence electrons introduces acceptor (p-type) or donor (n-type) conductivity, respectively, thereby modifying the material's electro-optical properties [6]. For effective doping, the size of the foreign atoms should ideally be within 15% of the host metal atoms to minimize lattice distortion. Previous studies have explored the doping of ZnSe with various elements, including Al [7], Ag [8], Pb [9], S [10], Cu [11], Mn [12], Ni [13], and Fe [14], to enhance its functional properties for specific applications. However, research on tin (Sn)-incorporated ZnSe thin films remains limited, despite the potential of Sn to modify the structural, optical, and electrical properties of ZnSe. Tin, with its unique electronic configuration, can act as a dopant to tune the bandgap and conductivity of ZnSe, making it a promising candidate for optoelectronic applications. To address this gap, this study investigates the effect of Sn incorporation at varying concentrations (0%, 2%, 4%, and 6%) on the structural, morphological, optical, and electrical

[1] Department of Electronics, Smt. G. G. Khadse College, Muktainagar, Jalgaon, Maharashtra, 425001 India.
[2] Department of Electronics,DNCVPS Shirish Madhukarrao Chaudhari College, Jalgaon, Maharashtra, 425001 India.

[*] Author to whom correspondence should be addressed: tahiramir13@gmail.com (T. A. H. Mir)

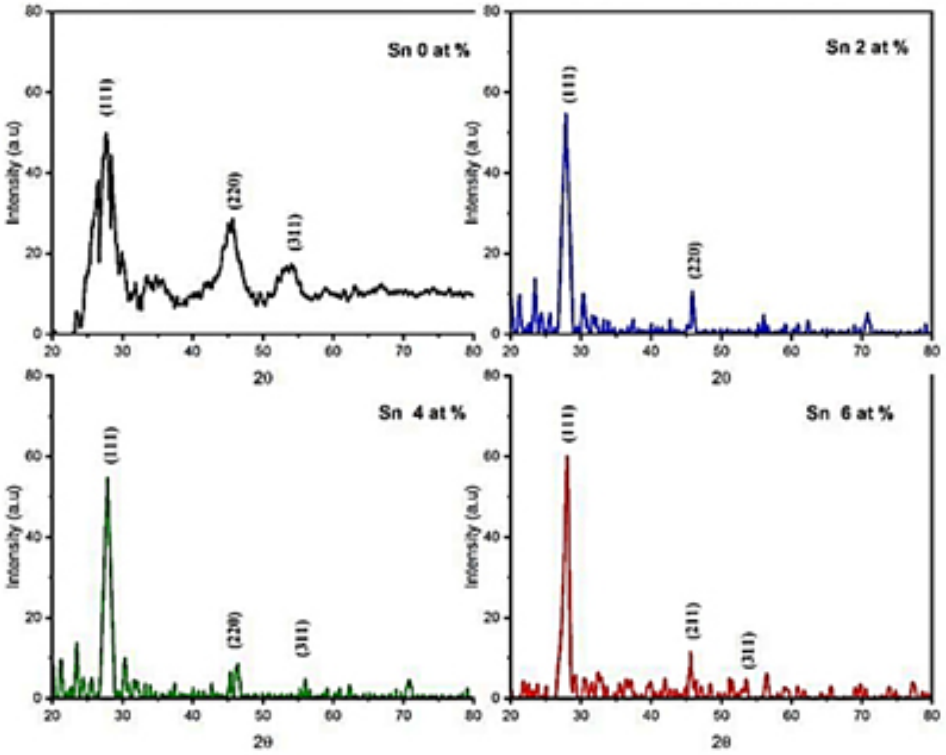

Fig. 1. XRD analysis of Sn incorporated ZnSe thin films for different concentrations of tin.

properties of ZnSe thin films synthesized via chemical bath deposition. This simple, cost-effective, and scalable method offers precise control over film composition and properties. The findings of this study aim to provide insights into the tunability of ZnSe thin films through Sn incorporation, paving the way for their application in next-generation optoelectronic devices.

2. EXPERIMENTAL

The synthesis of tin (Sn)-incorporated zinc selenide (ZnSe) thin films was carried out using a chemical bath deposition (CBD) technique. The process began with the preparation of a 100 mL stock solution of sodium selenosulfate (Na_2SeSO_3), which served as the source of Se^{2-} ions. This solution was prepared by refluxing 2.5 g of selenium powder with 7.5 g of sodium sulfite (Na_2SO_3) in deionized water at 80°C for 8 hours under continuous stirring. The resulting sodium selenosulfate solution was stored in an airtight container and used within two days to prevent aging, as direct use of selenium powder often leads to incomplete dissolution and residual impurities in the final product [15].

For the deposition of ZnSe thin films, a 0.5 M solution of zinc sulfate monohydrate ($ZnSO_4 \cdot H_2O$) was prepared in 10 mL of deionized water. To this solution, 8-10 mL of hydrazine hydrate (80%) was added slowly, causing the solution to transition from transparent to milky turbid due to the formation of zinc hydroxide ($Zn(OH)_2$). The solution was then stabilized by adding ammonia until it became transparent again, achieving a final pH of approximately 11.

To incorporate tin into the ZnSe matrix, tin chloride ($SnCl_2$) was used as the Sn source. Different concentrations of Sn (0%, 2%, 4%, and 6% by weight) were added to the zinc sulfate precursor solution. The deposition process was initiated by adding 20 mL of 0.25 M sodium selenosulfate to the reaction bath. The total volume was adjusted to 100 mL using deionized water, and the reaction was carried out at 65°C for 180 minutes under continuous stirring. After deposition, the substrates were rinsed with deionized water to remove loosely adhered particles and dried naturally in air. To enhance crystallinity, all films were annealed at 200°C for 1 hour before characterization.

The structural properties of Sn-incorporated ZnSe thin films were investigated using X-ray diffraction (XRD) analysis. The measurements were performed on a Philips PW3710 X-ray diffractometer equipped with Cu Kα radiation ($\lambda = 1.54056$ Å), with the 2θ range set from 20° to 80°. The morphological and elemental composition of the thin films were analyzed using a Scanning Electron Microscope (SEM, JEOL JED-2300, Japan) coupled with

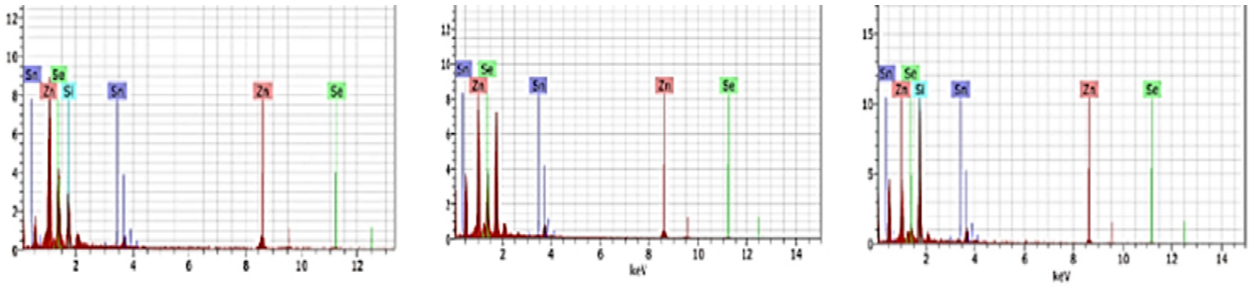

Fig. 2. EDS spectra of Sn incorporated ZnSe thin films at various concentration levels of tin.

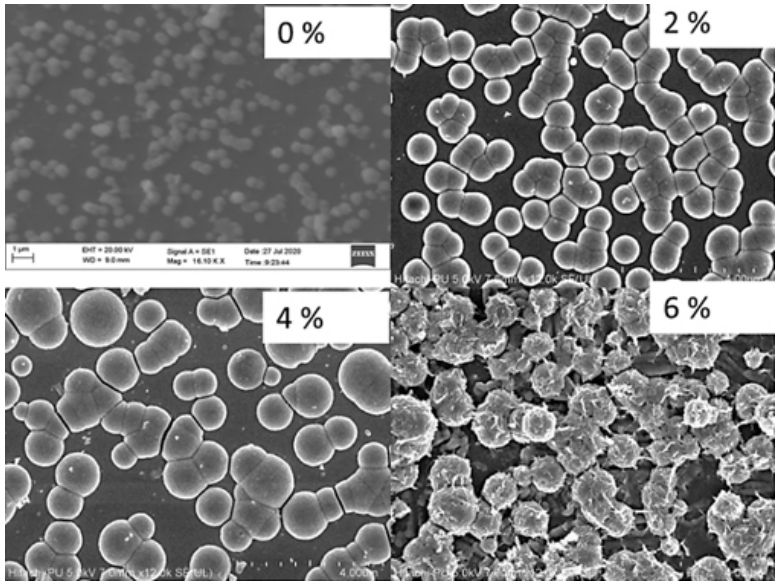

Fig. 3. Surface morphology of pure and tin incorporated zinc selenide thin films at various concentration levels of tin.

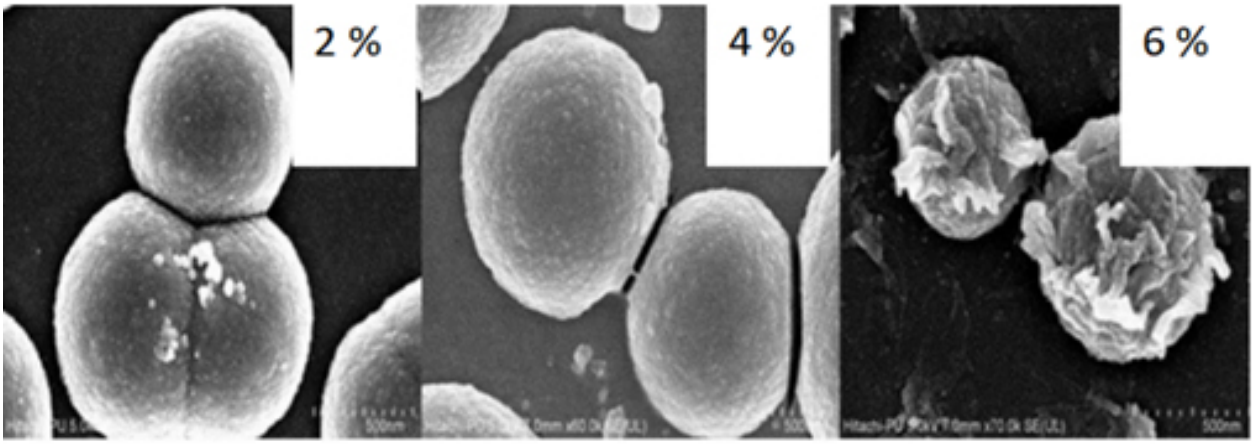

Fig. 4. urface morphology of pure and tin incorporated zinc selenide thin films at various concentration levels of tin at High magnitude (500nm).

Energy-Dispersive X-ray Spectroscopy (EDAX). Optical transmission spectra of the films were recorded in the wavelength range of 350-900 nm using a UV-Vis-NIR spectrophotometer (UV-3600, SHIMADZU).

The electrical resistivity of both pure and Sn-incorporated ZnSe thin films with varying Sn concentrations was measured using the DC two-probe method. For electrical contacts, silver paste electrodes were applied 1 cm apart on the film surface. The resistivity measurements were conducted over a temperature range of 300 K to 425 K, and the current was measured using a high-precision pico-ammeter.

3. RESULTS AND DISCUSSIONS

3.1 Structural Characterization

The X-ray diffraction (XRD) patterns of Sn-incorporated zinc selenide (ZnSe) thin films with varying doping concentrations, recorded in the 2θ range of 20°-80°, are depicted in Figure 1. The diffraction peaks observed at 27.33°, 45.45°, and 54.43° are indexed to the (111), (220), and (311) crystallographic planes, respectively, confirming the formation of a cubic phase with a preferred orientation along the (111) direction [JCPDS data file No. 80-0021]. Notably, the (220) and (311) peaks in Sn-incorporated thin films exhibit significantly lower intensity compared to their pure ZnSe counterparts. However, the intensity of the dominant (111) peak remains relatively unchanged across pure and Sn-incorporated samples. With increasing tin concentration, a slight narrowing of the dominant (111) peak is observed, indicating enhanced crystallinity and an increase in grain size. The structural parameters derived from the XRD analysis, including the full width at half maximum (FWHM) and d-spacing of the prominent (111) peak, are summarized in Table 1.

Table 1. XRD data analysis of Sn incorporated ZnSe thin films for various concentrations of tin.

Samples	2θ (deg)	Planes (h k l)	FWHM (β) (rad)	d (Å)
At 0% Sn	27.33	111	0.021	3.2624
At 2% Sn	27.83	111	0.016	3.2019
At 4% Sn	27.83	111	0.015	3.2019
At 6% Sn	27.95	111	0.012	3.1888

The average crystallite size (D) of the Sn-incorporated ZnSe thin films was calculated using the Debye-Scherrer formula, considering the (111) diffraction peak.

$$D = \frac{0.94\lambda}{\beta \cos\theta} \tag{1}$$

The interplanar spacing (d) was estimated by using Bragg's relation,

$$d = \frac{\lambda}{2\sin\theta} \tag{2}$$

As the obtained films exhibit cubic structure, the lattice parameter (a) was calculated by the following relation,

$$\frac{1}{d^2} = \frac{h^2 + k^2 + l^2}{a^2} \tag{3}$$

Here, h, k, l are lattice planes. The dislocation density was calculated using the following relation.

$$\delta = \frac{15\beta \cos\theta}{4aD} \tag{4}$$

The strain (ε) in the films was calculated from the relation,

$$\varepsilon = \frac{\beta \cos\theta}{4} \tag{5}$$

The grain size, lattice parameter, strain and dislocation density of tin films are summarized in Table 2. The dislocation density and strain were found to be decreased with a rise in tin content in the films indicating an improvement in the crystallinity. The grain size is observed to be increased from 6.85 nm to 9.55 nm with a rise in tin doping level. The enhancement in grain size with an increase in tin content in the films was reported earlier [16].

3.2 Elemental and Morphological Characterization

The composition of films can be determined by scanning a large area on the film by EDAX (Energy Dispersive X-ray Spectrum) of tin incorporated zinc selenide thin films with different concentrations of tin (2 %, 4 % and 6 %) are depicted in Figure 2. Additional peaks seen in the spectra are attributed to elements like oxygen, silicon, calcium, etc. of the glass substrate. The existence of Sn, Zn and Se elements are confirmed by the peaks present

in the EDS spectra. The surface morphology of Sn-doped zinc selenide (ZnSe) thin films at various tin doping concentrations was investigated using scanning electron microscopy (SEM). Figure 3 and Figure 4 present the SEM images of the films at lower and higher magnifications (500 nm), respectively. At lower tin concentrations, the films exhibit a microstructure characterized by symmetric and spherical microspheres. However, as the tin concentration increases, the microspheres lose their symmetry and spherical shape, becoming increasingly distorted. Notably, at a tin concentration of 6%, the microspheres exhibit significant morphological changes. Additionally, it is observed that the number of voids in the films decreases with increasing tin concentration, with the 6% Sn-doped films showing fewer voids compared to both pure ZnSe and films with lower Sn concentrations.

3.3 Optical Characterization

The optical transmittance spectra of Sn-doped zinc selenide (ZnSe) thin films with varying tin concentrations were recorded in the spectral range of 300–900 nm at room temperature, as illustrated in Figure 5.

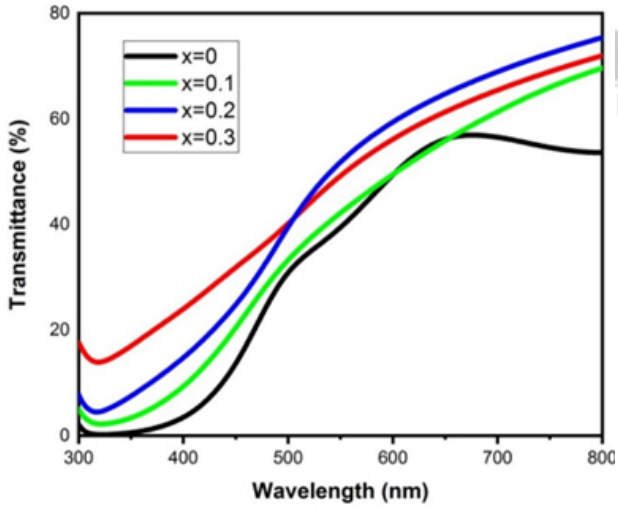

Fig. 5. Transmittance spectra of pure and tin incorporated zinc selenide thin films with various concentrations of tin.

Undoped ZnSe thin films exhibit higher transmittance compared to their Sn-doped counterparts. With increasing tin content, the transmittance spectra shift towards lower energy (higher wavelength) in the visible region, indicating a redshift. Furthermore, the transmittance decreases progressively with higher tin doping concentrations, suggesting an increase in absorbance. This reduction in transparency may be attributed to the enhanced film thickness resulting from the incorporation of tin. The increased absorbance in the visible region makes these films suitable for use as absorber layers in solar cell applications. A similar trend of reduced transmittance with increasing Sn doping concentrations has been reported for tin-doped zinc oxide films [17, 18]. In contrast, other studies on Sn-doped zinc oxide and cadmium selenide films have shown an increase in transmittance at higher Sn doping levels [19, 20], highlighting the material-dependent optical behavior of Sn-doped semiconductor films. The transition from the valence to the conduction band is given by the fundamental absorption depicted by the following relation and it helps to find out the bandgap of the films. The band gap was obtained using the following relation [21].

$$\alpha = \frac{A(h\nu - E_g)^n}{h\nu} \tag{6}$$

Where α is the absorption coefficient, A is a constant. n is equal to $\frac{1}{2}$ for direct bandgap semiconductor.

The energy intercept of the plot $(\alpha h\nu)^2$ versus $h\nu$ as shown in Figure 6 gives the band gap for the direct transition.

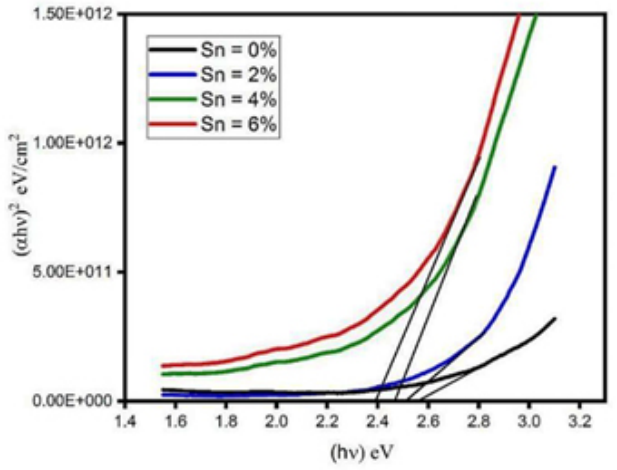

Fig. 6. GPlot of $(\alpha h\nu)^2$ versus $h\nu$ of pure and tin incorporated zinc selenide thin films at various concentration levels of tin.

The bandgap is found to be decreased from 2.57 eV for the pure film to 2.38 eV as the concentration of Sn is increased to 6%. Similar observations of decrease in band gap energy with increase in Sn concentration is reported for Sn doped ZnTe and CdSe films respectively [22, 23]. It was observed that the value of band gap decreases with Sn concentration. As concentration increases whether n-type or p-type, the impurity bands overlap with conduction or valence band giving rise to band tail and reduction in band gap is observed [6, 24].

Table 2. Grain size, lattice parameter, strain and dislocation density of Sn ZnSe thin films at tin concentrations.

Samples	Grain size (nm)	Lattice parameter (Å)	Strain ($\times 10^{-3}$)	Dislocation density ($10^{16}/m^2$)
At 0% Sn	6.85	5.6505	5.28	2.13
At 2% Sn	9.2	5.5458	3.89	1.15
At 4% Sn	9.4	5.5458	3.84	1.12
At 6% Sn	11.7	5.5225	3.08	0.72

3.4 Electrical Characterization

The variation of electrical resistivity with the temperature at the cooling time for various concentration levels of tin was presented in Figure 7.

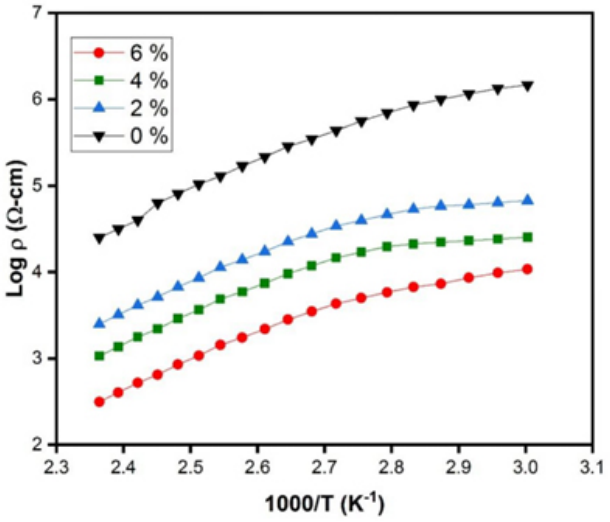

Fig. 7. Variations of $(\log \rho)$ with $1000/T$ for pure and tin incorporated zinc selenide thin films at various concentration levels of tin.

At room temperature, the resistivity values decreased from 10^6 to 10^3 Ω.cm as the concentration level increased from 0% to 6%. From the graph, it is evident that resistivity decreases with an increase in temperature confirming semiconducting nature. It is worth noting that the rise in the doping level of tin causes a decrease in the resistivity of thin films. This decrease in resistivity may be due to the decrease in defects and dislocations present in pure and lower concentrations of Sn incorporated films [23][23]. This is clear from XRD data presenting a fall in dislocation density and strain as tin concentration increases in the films. The low resistivity i.e high conductivity is one of the desirable properties of nanostructures for utilization in various solar cell applications.

4. CONCLUSION

Tin incorporated zinc selenide thin films have been synthesized by a convenient chemical bath deposition method for various concentration levels of tin. XRD studies revealed that with an increase in concentration of tin, there is a slight narrowing of prominent diffraction peaks suggesting improved crystallinity and grain size. EDAX studies confirmed the existence of Sn, Zn and Se elements by the corresponding peaks present in the EDS spectra. The transmittance curves showed a redshift of absorbance edge with an increase in tin content. With an increase in the concentration of tin, there is a fall in transmittance observed. The electrical resistivity was found to be decreased from 10^6 to 10^3 Ω.cm with the increase in concentration levels of tin. A decrease in bandgap energy is observed from 2.57 eV to 2.38 eV as tin content increases in the ZnSe films. The concentration of tin in zinc selenide thin films thus assists in tuning the bandgap and electrical resistivity as well to a wider range to facilitate its use in solar cell applications.

ACKNOWLEDGEMENT

The authors gratefully acknowledge the financial support provided by the Vice-Chancellor Research Motivational Scheme (VCRMS) of Kavayitri Bahinabai Chaudhari North Maharashtra University (Grant No. NMU/11A/VCRMS/2016-17/Science1/85), which enabled the successful completion of this work.

DECLARATIONS

Ethical Approval

We affirm that this manuscript is an original work, has not been previously published, and is not currently under consideration for publication in any other journal or conference proceedings. All authors have reviewed and approved the manuscript, and the order of authorship has been mutually agreed upon.

Funding

Vice-Chancellor Research Motivational Scheme (VCRMS) of Kavayitri Bahinabai Chaudhari

North Maharashtra University (Grant No. NMU/11A/VCRMS/2016-17/Science1/85)

Availability of data and material

All of the data obtained or analyzed during this study is included in the report that was submitted.

Conflicts of Interest

The authors declare that they have no financial or personal interests that could have influenced the research and findings presented in this paper. The authors alone are responsible for the content and writing of this article.

Authors' contributions

All authors contributed equally in the preparation of this manuscript.

REFERENCES

[1] Shirakawa, T., **2002**. . *Materials Science and Engineering B*, 91, p.470-474. https://doi.org/10.1016/S0921-5107(01)01006-6.

[2] Godlewski, M., Guziewicz, E., Kopalko, K., Łusakowska, E., Dynowska, E., Godlewski, M.M., Goldys, E.M. and Phillips, M.R., **2003**. Luminescence properties of ZnSe-based materials. *Journal of Luminescence*, 102-103, p.455-459. https://doi.org/10.1016/S0022-2313(02)00597-5.

[3] Lour, W.-S. and Chang, C.-C., **1996**. . *Solid-State Electronics*, 39, p.1295-1298. https://doi.org/10.1016/0038-1101(96)00033-0.

[4] Ullrich, B, **1998**. Comparison of the photocurrent of ZnSe/InSe/Si and ZnSe/Si heterojunctions. *Materials Science and Engineering: B*, 56(1), p.69-71. https://doi.org/10.1016/S0921-5107(98)00178-0.

[5] Yan, L. and Woollam, J. A. and Franke, E., **2002**. . *Journal of Vacuum Science and Technology A*, 20, p.693-701. https://doi.org/10.1116/1.1463085.

[6] Sharma, K. and Al-Kabbi, A. S. and Saini, G. S. S. and Tripathi, S. K., **2013**. Indium doping induced modification of the structural, optical and electrical properties of nanocrystalline CdSe thin films. *Journal of Alloys and Compounds*, 564, p.42-48. https://doi.org/10.1016/j.jallcom.2013.02.037.

[7] Kayed, T. S. and Qasrawi, A. F. and Elsayed, K. A., **2019**. Structural, optical, dielectric and electrical properties of Al-doped ZnSe thin films. *Journal of Electronic Materials*, 48(6), p.3519-3526. https://doi.org/10.1007/s11664-019-07055-3.

[8] Xi, Yang and others, **2015**. Solution-based Ag-doped ZnSe thin films with tunable electrical and optical properties. *Journal of Materials Chemistry C*, 3(38), p.9781-9788. https://doi.org/10.1039/C5TC01951F.

[9] Mita, Yoh and others, **2003**. PL characteristics of MBE-grown, Pb-doped ZnSe crystal layers. *Journal of Crystal Growth*, 251, p.576-580. https://doi.org/10.1016/S0022-0248(02)02482-X.

[10] Shaaban, E. R. and others, **2018**. Structural, optical and electrical characteristics of sulfur incorporated ZnSe thin films. *Optik*, 164, p.527-537. https://doi.org/10.1016/j.ijleo.2018.03.001.

[11] Wu, Yan and others, **2019**. Facile synthesis and color conversion of Cu-doped ZnSe quantum dots in an aqueous solution. *Journal of Materials Science: Materials in Electronics*, 30(24), p.21406-21415. https://doi.org/10.1007/s10854-019-02519-y.

[12] Acharya, Shinjita and others, **2010**. An alternate route to high-quality ZnSe and Mn-doped ZnSe nanocrystals. *Journal of Physical Chemistry Letters*, 1(2), p.485-488. https://doi.org/10.1021/jz900291a.

[13] Yadav, Kanta and Dwivedi, Yadav and Jaggi, Neena, **2015**. Structural and optical properties of Ni doped ZnSe nanoparticles. *Journal of Luminescence*, 158, p.181-187. https://doi.org/10.1016/j.jlumin.2014.09.025.

[14] Lohar, G. M. and others, **2015**. Studies of properties of Fe^{3+} doped ZnSe nanoparticles and hollow spheres for photoelectrochemical cell application. *Journal of Alloys and Compounds*, 653, p.22-31. https://doi.org/10.1016/j.jallcom.2015.08.208.

[15] Duan, Yu-lu and others, **2014**. Characterization of ZnSe microspheres synthesized under different hydrothermal conditions. *Transactions of Nonferrous Metals Society of China*, 24(8), p.2588-2597. https://doi.org/10.1016/S1003-6326(14)63387-2.

[16] Ikhioya, I. L. and Nkele, A. C. and Okoli, D. N. and Ekpunobi, A. J. and Ahmed, I., **2022**. Influence of varying molar concentration on the properties of electrochemically-deposited zirconium-doped ZnSe. *Journal of the Indian Chemical Society*, 99(9), p.100641. https://doi.org/10.1016/j.jics.2022.100641.

[17] Ajili, Mejda and Castagné, Michel and Turki, Najoua Kamoun, **2013**. Study on the doping effect of Sn-doped ZnO. *Superlattices and Microstructures*, 53, p.213-222. https://doi.org/10.1016/j.spmi.2012.10.012.

[18] Ganesh, V. and others, **2017**. Sn-doped ZnO nanocrystalline thin films with enhanced linear and nonlinear optical properties. *Journal of Physics and Chemistry of Solids*, 100, p.115-125. https://doi.org/10.1016/j.jpcs.2016.09.022.

[19] Bedia, Fatima Zohra and others, . Effect of tin doping on optical properties of nanostructured ZnO, journal = Journal of Alloys and Compounds, volume = 616, pages = 312-318, year = 2014, doi = 10.1016/j.jallcom.2014.07.086. .

[20] Dhanasekaran, V. and others, **2012**. Electrochemical synthesis and characterization of CdSnSe thin films. *Journal of Materials Science: Materials in Electronics*, 23(2), p.645-651. https://doi.org/10.1007/s10854-011-0463-1.

[21] Garadkar, K. M. and Patil, A. A. and Hankare, P. P. and Chate, P. A. and Sathe, D. J. and Delekar, S. D., **2009**. MoS2: Preparation and characterization. *Journal of Alloys and Compounds*, 487(1-2), p.786-789. https://doi.org/10.1016/j.jallcom.2009.08.069.

[22] Pandey, Neha and Kumar, Brijesh and Dwivedi, D. K., **2019**. Synthesis and characterization of pure and Sb/Sn doped ZnTe. *Materials Research Express*, 6(9), p.096425. https://doi.org/10.1088/2053-1591/ab2fb8.

[23] Sahu, Prashant K. and Das, R. and Lalwani, Rajesh, **2018**. Incorporation of tin in nanocrystalline CdSe thin films. *Applied Physics A*, 124(10), p.665. https://doi.org/10.1007/s00339-018-2094-3.

[24] Sharma, K. and Al-Kabbi, A. S. and Saini, G. S. S. and Tripathi, S. K., **2015**. Influence of Zn doping on structural, optical and electrical properties of nanocrystalline CdSe. *Journal of Alloys and Compounds*, 651, p.42-48. https://doi.org/10.1016/j.jallcom.2015.08.038.

